Original Research Article

Enhanced chemotherapeutic behavior of open-caged DNA@Doxorubicin nanostructures for cancer cells†

Vinit Kumar[1], Samer Bayda[1,2], Mohamad Hadla[1,3], Isabella Caligiuri[1], Concetta Russo Spena[1], Stefano Palazzolo[1,2], Susanne Kempter[4], Giuseppe Corona[1], Giuseppe Toffoli[1] and Flavio Rizzolio[1]*

[1] Clinical Pharmacology, Department of Molecular Biology and Translational Research, National Cancer Institute and Center for Molecular Biomedicine, CRO Aviano (PN),
Via Franco Gallini, 2, AVIANO 33081 - PN - Italy
[2] Doctoral School in Nanotechnology, University of Trieste, Italy
[3] Doctoral School in Pharmacological Sciences, University of Padua, Italy
[4] Faculty of Physics and Center for Nanoscience, Ludwig-Maximilians-Universität München, München, Germany.

*Correspondence: Flavio Rizzolio, PhD
Clinical Pharmacology, Department of Molecular Biology and Translational Research, National Cancer Institute and Center for Molecular Biomedicine, CRO Aviano (PN),
Via Franco Gallini, 2, AVIANO 33081 - PN - Italy
tel. +39-0434 659384
fax. +39-0434 659799
e-mail: *frizzolio@cro.it*

Keywords: DNA nanotechnology, drug delivery, cancer therapy, nanomedicine, doxorubicin

Contract grant sponsor: My First AIRC; Contract grant number: 1569.
Contract grant sponsor: AIRC Special Program Molecular Clinical Oncology, 5x1000; Contract grant number: 12214.
Contract grant sponsor: Italian Ministry of Education MIUR; Contract grant number: prot.RBAP11ETKA.

Additional Supporting Information may be found in the online version of this article.

Received 22 March 2015; Revised 7 May 2015; Accepted 26 May 2015
Journal of Cellular Physiology

DOI 10.1002/jcp.25057

ABSTRACT

In cancer therapy, it is imperative to increase the efficacy and reduce side effects of chemotherapeutic drugs. Nanotechnology offers the unique opportunity to overcome these barriers. In particular, in the last few years DNA nanostructures have gained attention for their biocompatibility, easy customized synthesis and ability to deliver drugs to cancer cells. Here, an open-caged pyramidal DNA@Doxorubicin (**Py-Doxo**) nanostructure was constructed with 10 DNA sequences of 26-28 nucleotides for drug delivery to cancer cells. The synthesized DNA nanostructures are sufficiently stable in biological medium. **Py-Doxo** exhibited significantly enhanced cytotoxicity of the delivered doxorubicin to breast and liver cancer cells up to two fold compared to free doxorubicin. This study demonstrates the importance of the shape and structure of the designed transporter DNA nanostructures for biomedical applications.

Introduction

It is estimated that about 30-60% of cancer patients receive drugs without any clinical benefit (La Thangue & Kerr, 2011). It is a challenging task for scientists and technologists to increase the efficacy and reduce side effects of chemotherapeutic drugs. Among chemotherapeutic drugs, doxorubicin (doxo) is used in many common tumors including breast, lung, lymphomas, multiple myeloma, ovarian, and prostate (Tacar et al., 2013). Doxo is an anthracycline antibiotic that intercalates in the DNA helix preventing replication (Gewirtz, 1999). However, doxo inheres some severe side effects including lipid peroxidation and free radical production that contribute to cardiac toxicity and cutaneous vascular effects. These effects are mainly due to its poor selectivity (Tacar et al., 2013). In this regard, nanotechnology represents a complementary and alternative approach to improve the treatment of cancer by overcoming the classical limitations of chemotherapeutic drugs including multi-drug resistance.

Recently, many research groups have focused their attention on DNA, a genetic material, which possesses minimal toxicity (Pinheiro et al., 2011). DNA has intrinsic and fascinating properties such as easy customized synthesis of strands with various length and functional groups, molecularly identical particle size, high loading efficiency, stability, effective cellular internalization, and biocompatibility (Pinheiro et al., 2011; Bhatia et al., 2011; Chang et al., 2011). For these reasons, DNA nanostructures are ideally suited for biomedical applications ranging from biosensing to drug delivery and provide excellent platforms for the development of highly nontoxic drug nano-carriers for cancer therapy (Bhatia et al., 2011; Chang et al., 2011; Li et al., 2013; Wang & Ding, 2014; Liu & Liu, 2009). It has been demonstrated that the activity of anticancer drugs could be regulated in cancer cells by loading/encapsulating them in DNA origami nanostructures with tailored shapes, sizes, and global twist (Jiang et al., 2012; Zhao et al., 2012). Although these data are very promising, in these studies relatively complex DNA nanostructures have been utilized. The research area of DNA nanostructures for drug delivery is still in its initial stages and more investigation is needed to fully realize their potential applications in the biomedical field. Herein, we have analyzed for the first time the drug

delivery efficiency of a rigid open-caged pyramidal DNA nanostructure **(Py)** on diverse cancer cells. The pyramidal DNA nanostructures are synthesized by annealing 10 DNA sequences adopted from the literature (Bhatia et al., 2009). We demonstrated that these easy structures could encapsulate doxo **(Py-Doxo)** and have excellent anticancer activity against breast and liver cancer cells. These simple DNA structures are also able to deliver doxo to cancer cells overexpressing multi-drug resistance proteins (Visentin et al., 2009).

RESULTS

Py is stable under physiologic conditions and slowly releases doxo

The final open-caged **Py** nanostructure was constructed by two-step synthetic protocol *i.e.*1) synthesis ofsingle modules A and B with five way junctions; 2) construction of the final structure by assembling the two modules **A** and **B**. The formation of **A** and **B** was confirmed by native PAGE (polyacrylamide gel electrophoresis) (Fig. S1). In the next step, equimolar solution of **A** and **B** were mixed in a 1:5 ratio and this mixture was annealed to obtain the final **Py** nanostructure. The formation of **Py** was confirmed and characterized by gel electrophoresis (Fig. 1). **Py** was purified by gel elution and confirmed by native PAGE and utilized in all the subsequent studies (Fig. 1).

For biological applications, the nanostructure should be able to resist specific and nonspecific degradations under physiological conditions (Schüller et al., 2011). We have analyzed the stability of **Py** in the presence of cell culture medium with 5% FBS. It is evident from this analysis that **Py** is stable enough up to 35 hours to enzymatic degradation under these cellular conditions and could be effectively used as drug delivery vehicle. The kinetics of degradation fit well to the first order exponential decay (r^2: 0.85) (Fig. 2). The calculated half-life of the **Py** is 34.5 hours (Conway et al., 2013).

Motivated by the result of stability test, we loaded **Py** with doxo to test **Py-Doxo** hybrid as drug delivery system. Doxo intercalates with double strand (ds) DNA through stacked-base-pair interactions. For doxo loading, **Py** nanostructure (98 ng/μL) was mixed with doxo (1mg/mL) at room temperature, incubated for 1 hour and then purified by centrifugation (Fig. S2). Doxo is a fluorescent molecule that can be easily quantified in samples by measuring the intrinsic fluorescence. The amount and efficiency of doxorubicin loaded into **Py** was calculated using a calibration curve obtained by the incubation of **Py** (98 ng/μL) with serially diluted doxo (from 1.0 mg/mL to 0.0625 mg/mL). The loading efficiency of doxo into **Py** was calculated according to equation 1.

$$Doxo\ loading\ efficiency = \frac{Doxo\ loaded\ to\ Py}{Initial\ doxo\ concentration} \times 100 \quad (1)$$

The loaded content of doxo increases with an increase in the initial amount of doxo used for intercalation (Fig. 3a). Doxo is known to undergo self-association in aqueous solution, which may alter binding and release properties of doxo from the nanocarrier (Agrawal et al., 2009; Karukstis et al., 1998). To avoid unspecific loading of doxo in the present case, we used **Py-Doxo** with a 15% loading efficiency of doxo. Roughly, 172 molecules of doxo were associated with a single **Py** nanostructure under this condition. The kinetics of doxo release from **Py** in PBS and FBS were evaluated (Fig. 3b). We calculated the release of doxo using a log-log plot of cumulative release *vs* time. Interestingly, 50% of doxo release from **Py-Doxo** in PBS and FBS was achieved in about 5 and 3 hours, respectively, whereas free doxo diffused quickly from a semipermeable membrane. In fact, 50% of doxo release occurred within 20 minutes.

Py increases the internalization of doxo in cancer cells

Two aggressive cell lines from breast (MDA-MB-231) and liver (HepG2) cancers were used to examine the ability of cellular internalization of **Py-Doxo**. We studied cell internalization of **Py-Doxo** by fluorescence microscopy analysis. **Py-Doxo** was probed with DAPI and shown in green (Fig. 4). As shown in Figure 4, **Py-Doxo** is able to penetrate inside MDA-MB-231 cells without any support of transfection agent. **Py** releases the doxo (red) in the nucleus to exert its cytotoxic activity. No signal was detected in the untreated cells (background). Quantification of drug internalization demonstrated that **Py-Doxo** was more effective than free doxo with an increase of 26% (p value< 0.01) (Fig. 5).

Py increases the cytotoxicity of doxo in cancer cells

Cell viability studies demonstrated that **Py-Doxo** reduced cell viability of MDA-MB-231 and HepG2 more than free doxorubicin. The difference between **Py-Doxo** and free-doxo is statistically significant at three different concentrations as shown in Figure 6. In MDA-MB-231 and HepG2 cell lines, the maximal percentage of inhibition was 49 and 51%, respectively. Interestingly, **Py-Doxo** and free-doxo had the same cytotoxic effects on normal cell lines (Fig. S3). Finally, we evaluated the effect of **Py-Doxo** in multi-drug resistance cell line. We used regular (LoVo) and doxorubicin-resistant (LoVo-R)

cells. In both cell lines, there was no statistically significant difference between **Py-Doxo** and free-doxorubicin (Fig. S4). In order to assess for the bio-compatibility of **Py**, we administered free **Py** to MDA-MB-231, HepG2, and LoVo cells and no obvious cytotoxicity was observed in these cell lines which again confirms excellent bio-compatibility of **Py** (data not shown).

CONCLUSIONS

Starting from a simple open-caged DNA nanostructure constructed from only 10 DNA sequences, we have prepared a new drug delivery system able to incorporate and release the chemotherapeutic drug doxorubicin as shown in Scheme 1. Doxo-intercalated Py exhibited efficient and enhanced internalization and antineoplastic effect. In comparison to DNA origami, Py is a simple, easy to construct, cost-effective, and nontoxic transporter for doxo for various cancer cell lines. Although **Py** is not a highly-dense DNA nanostructure, it is stable in biological solutions and gives us a proof of concept system able to kill cancer cells. Interestingly, the cytotoxic behavior of **Py-Doxo**, which is an open-caged structure, is significantly different from the caged DNA nanostructures such as icosahedron and tetrahedron. DNA icosahedron/doxo showed higher cytotoxicity compared to free doxorubicin on MCF-7 cells only after functionalization with a tumor-targeting aptamer sequence (Jiang et al., 2012). DNA tetrahedron/doxo exhibited higher cytotoxicity on doxo resistant MCF-7/ADR cells (Kim et al., 2013). The marked difference in the structure of the **Py** compared to those of previously reported caged DNA nanostructures is likely to be responsible for the observed behavior. In a biological system, nanostructures interact with the cellular components (nucleus, membrane, mitochondria) to exert their cytotoxic effect, which ultimately inhibits tumor progression and growth (Eckhardt et al., 2013). Recent investigations have concluded that the cellular interaction and cytotoxicity of nanostructure based drug transporters depends strongly on their size, shape, and charge (Kim et al., 2013; Lewinski et al., 2008). DNA nanostructures have ideally some advantages compare to other well-developed drug delivery systems. Doxil, a PEGylated-liposomal formulation of doxorubicin, is one of a few cases of success in clinics, which improves the circulation time of doxo. Although the *in vivo* stability of DNA nanostructures is still a limitation, it could be tuned and optimized by the judicious selection of the shape and size, programmable and controllable, and non-toxic. In comparison, at present, the field of DNA nanotechnology for drug delivery is still under developed but in the long term could be of help for the patients. We envision that these DNA structures could elevate the cytotoxic effect and efficacy

of the drug by increasing the effective local concentration at the pathologic site. We believe that our study will be helpful for tuning the design of prospective DNA nanostructures with optimal performance for biomedical applications.

Materials and Methods

Reagents

All DNA sequences were purchased from IDT technologies and used without further purification (Table 1). Final concentration of all strands were adjusted to 100 μM and used as stock. Chemicals: Doxo solution (2mg/mL) from Pfizer; polyacrylamide/Bis solution (19:1) 40% from BioRad; *N*, *N*, *N*', *N*'-Tetramethylethylenediamine (TEMED), Ammoniumpersulfate (APS), ethidium bromide from Sigma-Aldrich; TAE 50x powder from Medicago. All the gels (native and agarose) were run in 1xTAE buffer (Tris-acetate/EDTA). In all the experiments, MilliQ water (millipore, 18.2 Ω) was used.

Synthesis of DNA nanostructures

Two modules A and B were synthesized by mixing the strands (A1 to A5) and (B1 to B5) in separate tubes in equimolar concentrations (10 μM) in the presence of 10 mM phosphate buffer (pH 6), 100 mM NaCl and 2 mM $MgCl_2$ in a final volume of 100 μl (Bhatia et al., 2011; Bhatia et al., 2009). The oligonucleotides were heated to 90 ^{o}C for 20 min and then cooled down to room temperature at a rate of 1°C/5min and equilibrated at 4°C for 72 h. Formation of A and B was confirmed by native PAGE (polyacrylamide gel electrophoresis). In the next step, a 1:5 ratio of A:B was mixed and heated to 50°C for 4h and samples were annealed at the rate of 1°C/5min at 20°C followed by incubation at 20°C for 2h, then equilibrated at 4°C for 72h to obtain the **Py** nanostructure. **Py** was purified by gel elution in a phosphate buffer, 2h at 80 V. Purification of **Py** was confirmed by native PAGE.

Stability of Py under different experimental conditions

5 μl of **Py** (45 ng μl^{-1}) was mixed with 5 μl of cell culture medium + 10% FBS (v/v) and incubated at 37°C for different hours (2, 8, 24, 26, 31 and 49). The stability of the **Py** nanostructure was analyzed on 1 % agarose gel.

Doxorubicin loading Efficiency and release

The amount and efficiency of doxo loaded into **Py-Doxo** was calculated by incubating **Py** (98 ng/μL) with serially diluted doxo (1mg/mL to 0.0625 mg/ mL) for 1 h at RT and then purified by centrifugation at 16000G for 15 min and washed two times. The loading efficiency of doxo into **Py-**

Doxo was calculated according to equation 1 (see results). The release of doxo and **Py-Doxo** (0.040mg/0.5mL) was evaluated with a dialysis membrane of 15000 MW dipped into 1L of PBS.

Doxorubicin internalization

MDA-MB-231 cells were seeded in a 24 multiwell plates at a density of $1x10^5$ cells/well. The following day, the cells were treated with doxo and **Py-Doxo** at a concentration of 1μg/mL, incubated for 2 h, and washed three times with PBS. Before treatment, **Py-Doxo** was incubated with DAPI for 5 min, centrifuged (10000rpm x 15min) and washed two times. The cells were imaged with a Leica fluorescence microscopy at 20x magnification. Fluorescence intensity was calculated by treating the cells with 500 ng/mL of doxo and **Py-Doxo** for two hours. The cells were imaged with a Leica fluorescence microscope at 20x magnification. The fluorescence signal was evaluated with the Nikon NIS Elements 4.1 software.

Cell Viability assay

The cytotoxicity of free doxo, **Py** and **Py-Doxo** was tested against breast MDA-MB-231, hepatic HepG2, and colon LoVo cancer cell lines. The cytotoxicity was evaluated by CellTiter-Glo® Luminescence assay (Promega) with the Infinite 200 PRO instrument (Tecan). Cells were grown accordingly to ATCC. Cells were seeded in 96-well plates (Falcon BD) at a density of 10^3 cells/well and incubated for 24 h to allow for cell attachment. The cells were incubated with doxo, **Py,** and **Py-Doxo** at the same drug concentrations for 96 hours. The cell viability rate was calculated by the following equation:

Cell viability rate (%) = (Ldrug -Lblank)/(Lcontrol - Lblank); Ldrug is the luminescence of the cells incubated with doxo or **Py-Doxo**; Lcontrol is the luminescence of the cells incubated with the vehicle or **Py**, respectively; and Lblank is the luminescence of the assay buffer.

Statistical Analysis

The statistical significance was determined using a t-test. A p-value less than 0.05 was considered significant for all comparisons. All data were expressed as mean ± SD.

Acknowledgment

Authors are thankful to AIRC Special Program Molecular Clinical Oncology, 5x1000, (No. 12214), My First AIRC (No. 1569), Italian Ministry of Education MIUR (FIRB prot.RBAP11ETKA) for funding.

Disclosure

Authors declare no conflicts of interest.

Literature Cited

Agrawal, P., Barthwal, S.K. & Barthwal, R., 2009. Studies on self-aggregation of anthracycline drugs by restrained molecular dynamics approach using nuclear magnetic resonance spectroscopy supported by absorption, fluorescence, diffusion ordered spectroscopy and mass spectrometry. *Eur. J. Med. Chem.*, 44(4), pp.1437–51.

Bhatia, D. et al., 2011. A synthetic icosahedral DNA-based host-cargo complex for functional in vivo imaging. *Nat. Commun.*, 2, p.339.

Bhatia, D. et al., 2009. Icosahedral DNA nanocapsules by modular assembly. *Angew. Chem. Int. Ed. Engl.*, 48(23), pp.4134–7.

Chang, M., Yang, C.-S. & Huang, D.-M., 2011. Aptamer-conjugated DNA icosahedral nanoparticles as a carrier of doxorubicin for cancer therapy. *ACS nano*, 5(8), pp.6156–63.

Conway, J.W. et al., 2013. DNA nanostructure serum stability: greater than the sum of its parts. *Chem. Commun. (Camb)*, 49(12), pp.1172–4.

Gewirtz, D.A., 1999. A critical evaluation of the mechanisms of action proposed for the antitumor effects of the anthracycline antibiotics adriamycin and daunorubicin. *Biochem. Pharmacol.*, 57(7), pp.727–41.

Jiang, Q. et al., 2012. DNA origami as a carrier for circumvention of drug resistance. *J. Am. Chem. Soc.*, 134(32), pp.13396–403.

Karukstis, K.K. et al., 1998. Deciphering the fluorescence signature of daunomycin and doxorubicin. *Biophys. Chem.*, 73(3), pp.249–63.

Kim, K.-R. et al., 2013. Drug delivery by a self-assembled DNA tetrahedron for overcoming drug resistance in breast cancer cells. *Chem. Commun. (Camb)*, 49(20), pp.2010–2.

Li, J. et al., 2013. Smart drug delivery nanocarriers with self-assembled DNA nanostructures. *Adv. Mater.*, 25(32), pp.4386–96.

Liu, H. & Liu, D., 2009. DNA nanomachines and their functional evolution. *Chem. Commun. (Camb)*, (19), pp.2625–36.

Pinheiro, A. V et al., 2011. Challenges and opportunities for structural DNA nanotechnology. *Nat. Nanotechnol.*, 6(12), pp.763–72.

Schüller, V.J. et al., 2011. Cellular immunostimulation by CpG-sequence-coated DNA origami structures. *ACS nano*, 5(12), pp.9696–702.

Tacar, O., Sriamornsak, P. & Dass, C.R., 2013. Doxorubicin: an update on anticancer molecular action, toxicity and novel drug delivery systems. *J. Pharm. Pharmacol.*, 65(2), pp.157–70.

La Thangue, N.B. & Kerr, D.J., 2011. Predictive biomarkers: a paradigm shift towards personalized cancer medicine. *Nat. Rev. Clin. Oncol.*, 8(10), pp.587–96.

Visentin, M. et al., 2009. Identification of proteins associated to multi-drug resistance in LoVo human colon cancer cells. *Int*. *J*. *Clin*. *Oncol*., 34(5), pp.1281–9.

Wang, Z.-G. & Ding, B., 2014. Engineering DNA Self-Assemblies as Templates for Functional Nanostructures. *Acc*. *Chem*. *Res*., *47* (6), pp 1654–1662

Zhao, Y.-X. et al., 2012. DNA origami delivery system for cancer therapy with tunable release properties. *ACS nano*, 6(10), pp.8684–91.

Legend to Figures

Fig. 1. Native 7% PAGE image showing the assembly of **Py**. Left lane shows the formation of modules **A** and **B**. Middle lane confirms the formation of **Py**. Right lane shows the purified **Py**.

Fig. 2. Kinetic analysis of **Py** degradation in medium with 5% FBS. Intensity of the bands was calculated by Photoshop software and corresponds to the amount of **Py** (Y axis) over the time (X axis).

Fig. 3. A) Loading efficiency of **Py-Doxo**. The graph displays the percentage of loading efficiency of doxo (Y axis) at different drug concentration (X axis). λ_{ex}465±35nm; λ_{em}595±25nm. B) Release of doxo from **Py**. The release of doxo was evaluated by measuring the fluorescence of doxo that resided inside the dialysis membrane at each time point. • Free-doxo (PBS), ▲ **Py-Doxo** (FBS), ■ **Py-Doxo** (PBS).

Fig. 4. Fluorescence analysis of **Py-Doxo** in MDA-MB-231 cells. Upper panel: cells were treated with **Py-Doxo** for 2 hours. The DNA nanostructure was marked with DAPI and showed in green. Doxo is autofluorescent and represented in red. Middle panel: cells were treated with free doxorubicin. Lower panel: cells were treated only with vehicle. Images were done at 20x magnification. Scale bar is 10 μm.

Fig. 5. Internalization of doxo in MDA-MB-231 cells. ** pvalue< 0.01.

Fig. 6. Effect of **Py-Doxo** on MDA-MB-231 and HepG2 cell viability. Cells were treated with increasing concentration of doxorubicin or **Py-Doxo** as indicated on the X axis (ng/ml). The cell viability values were normalized as doxo/vehicle or **Py-Doxo**/**Py**. * pvalue<0.05 (Y axis). **Py-Doxo** is more efficient than free doxo at all concentrations.

Scheme 1. Schematic representation for the synthesis, loading and delivery of **Py-Doxo** to the cells and depicting the internalization of **Py-Doxo** hybrid and the release of doxo.

Table 1. Oligonucleotides utilized to assemble A (from A1 to A5) and B (from B1 to B5).

A1	GC CTG GTG CC ACC GGT GA CGT TCC GC
A2	GC CTG GTG CC CCG CGT CC TCA CCG GT
A3	GC CTG GTG CC GCC ACG CT *TT* GGA CGC GG
A4	GC CTG GTG CC GCG AGT GC *AA* AGC GTG GC
A5	GC CTG GTG CC GCG GAA CG *AA* GCA CTC GC
B1	CA TCA GTC GC ACC GGT GA CGT TCC GC
B2	TT ATA GGA CT CCG CGT CC TCA CCG GT
B3	TT ATA GGA CT GCC ACG CT *TT* GGA CGC GG
B4	GC GAC TGA TG GCG AGT GC *AA* AGC GTG GC
B5	GG CAC CAG GC GCG GAA CG *AA* GCA CTC GC

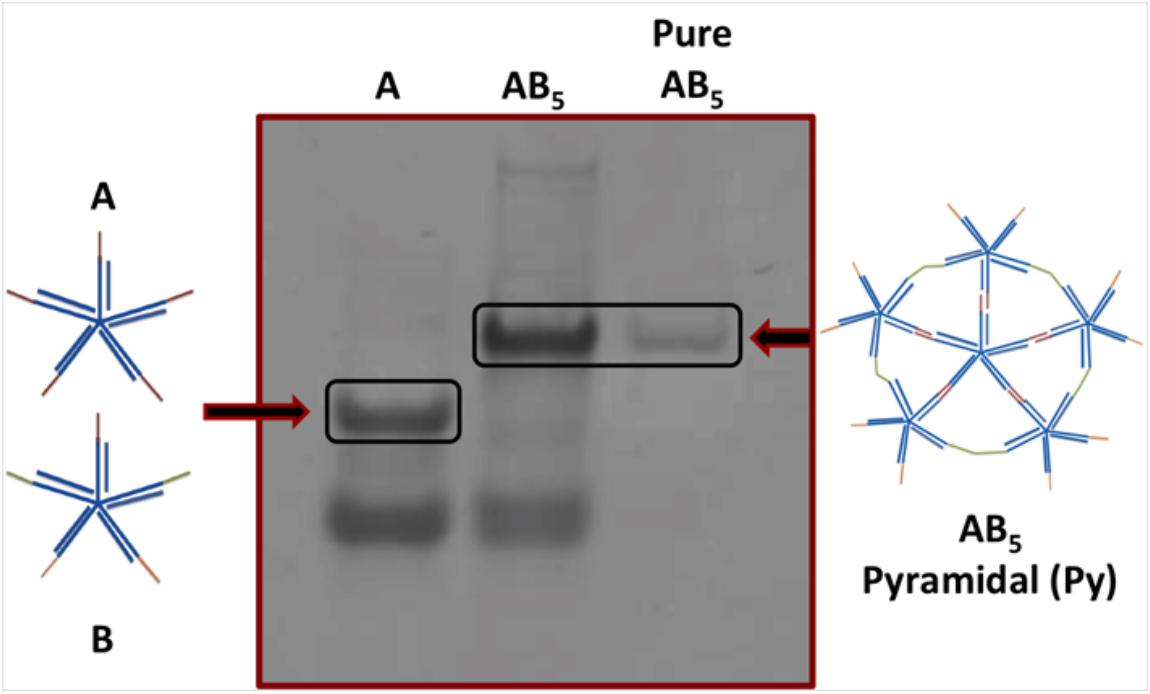

Figure 1

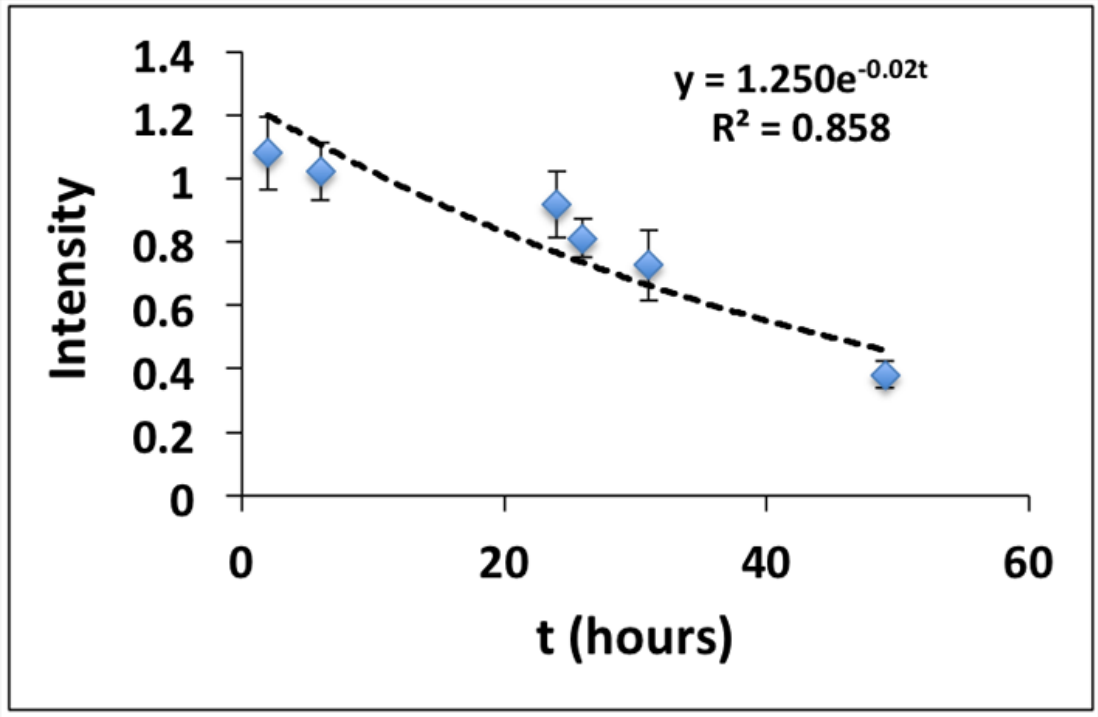

Figure 2

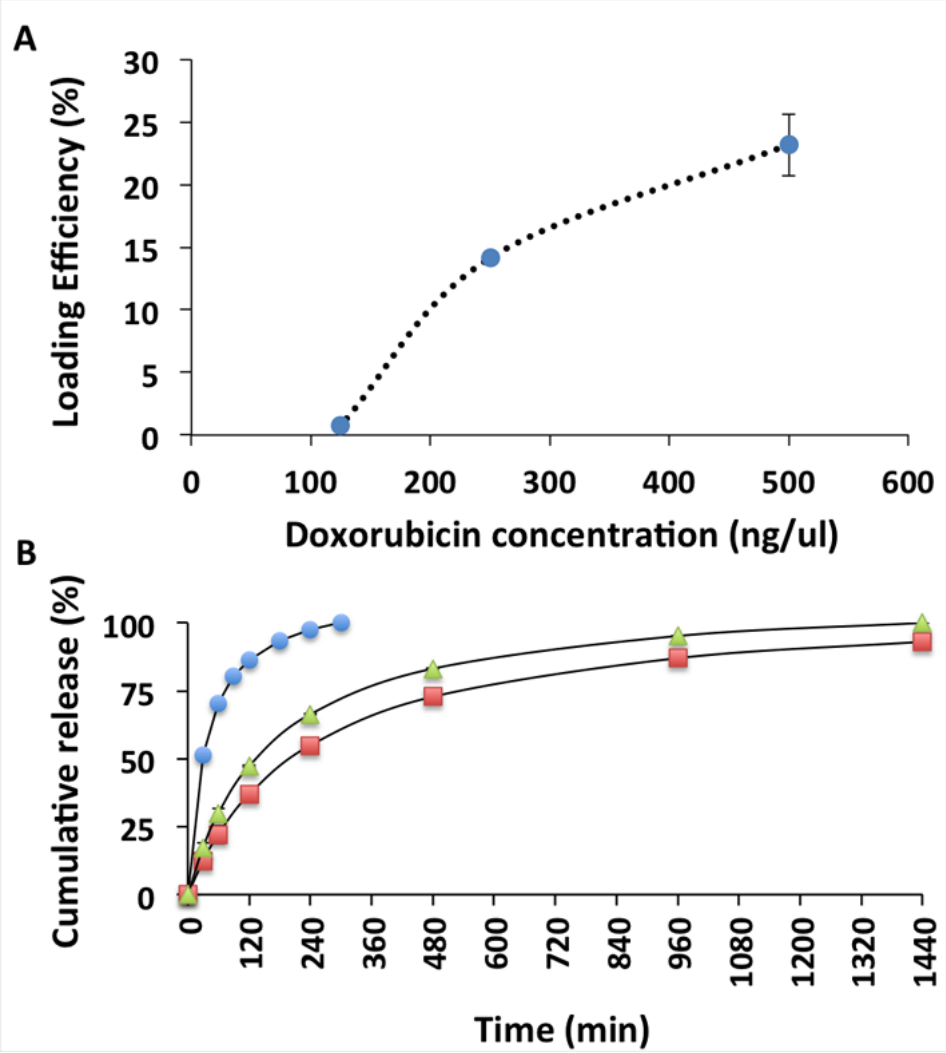

Figure 3

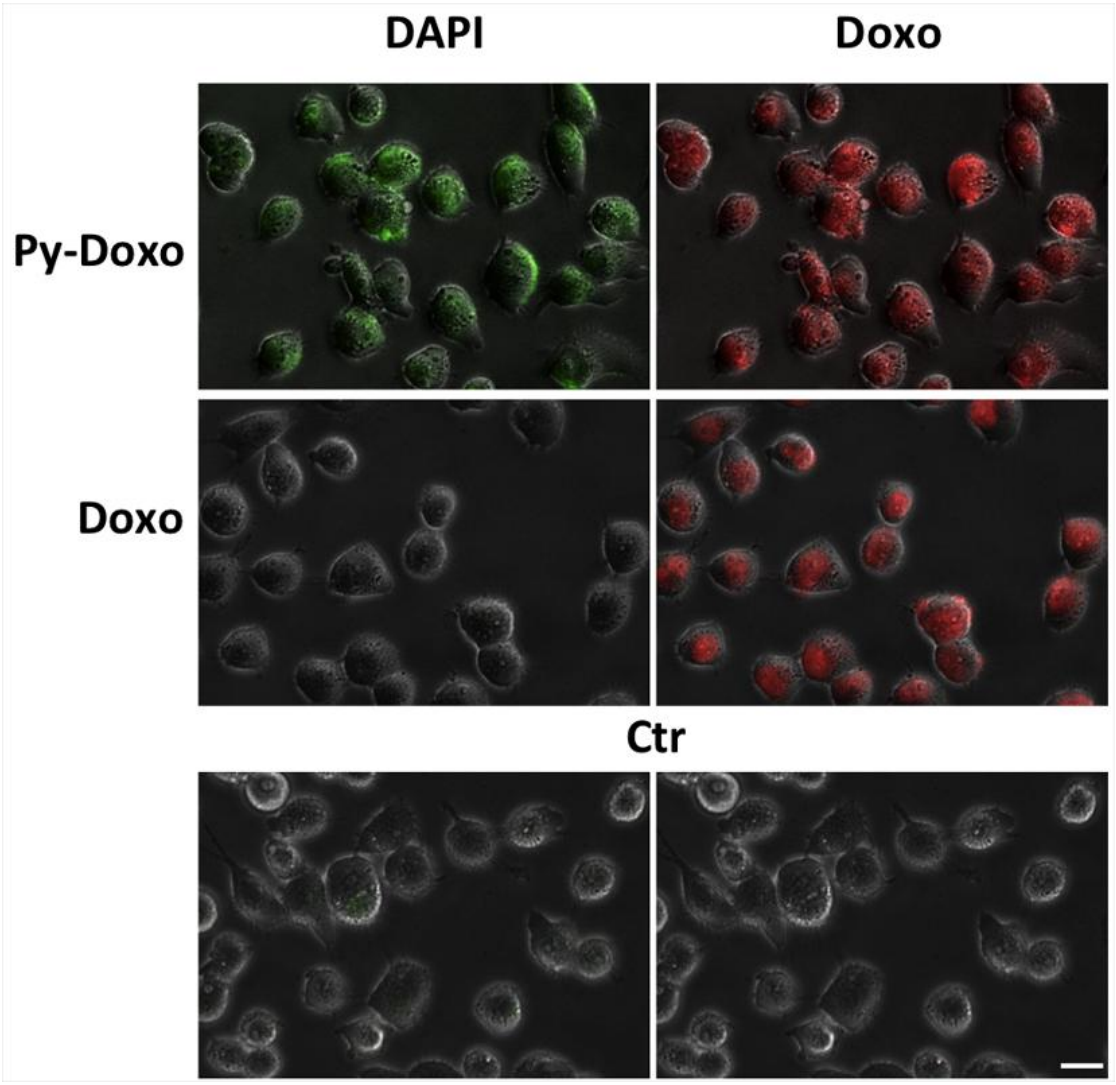

Figure 4

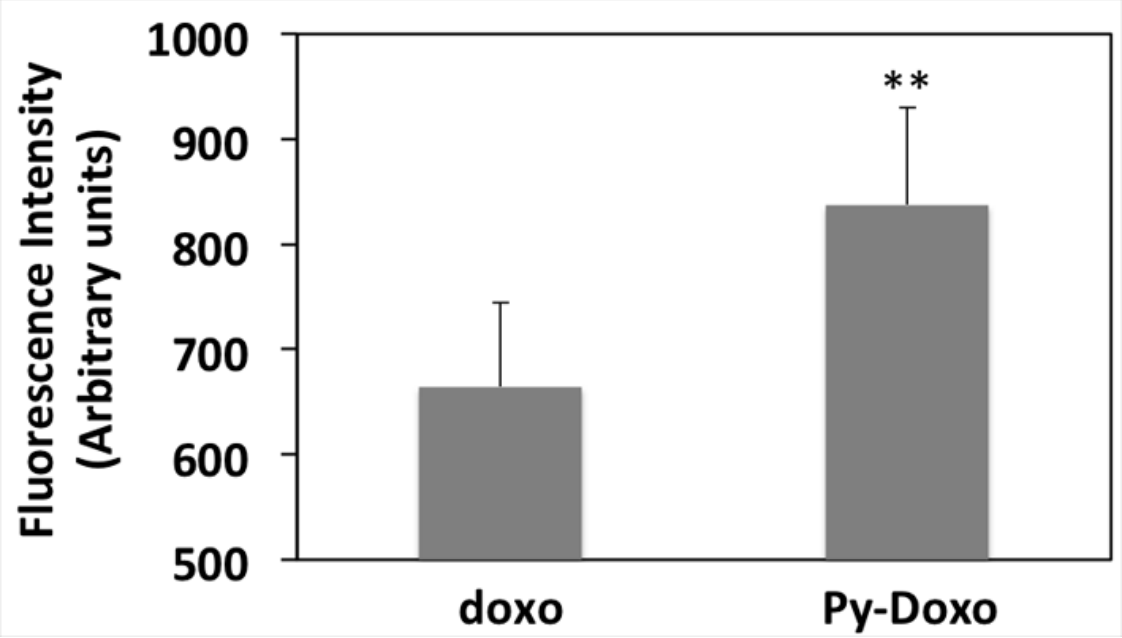

Figure 5

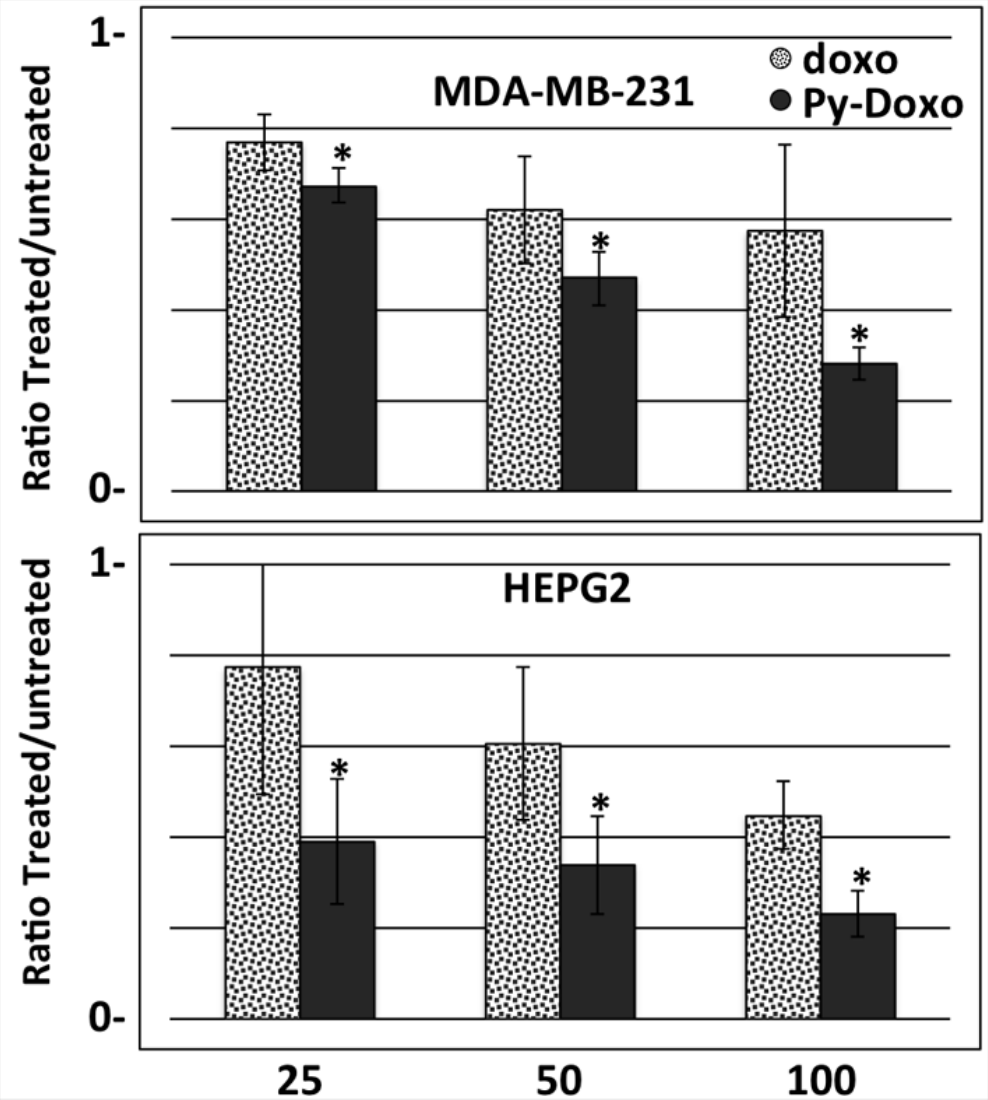

Figure 6

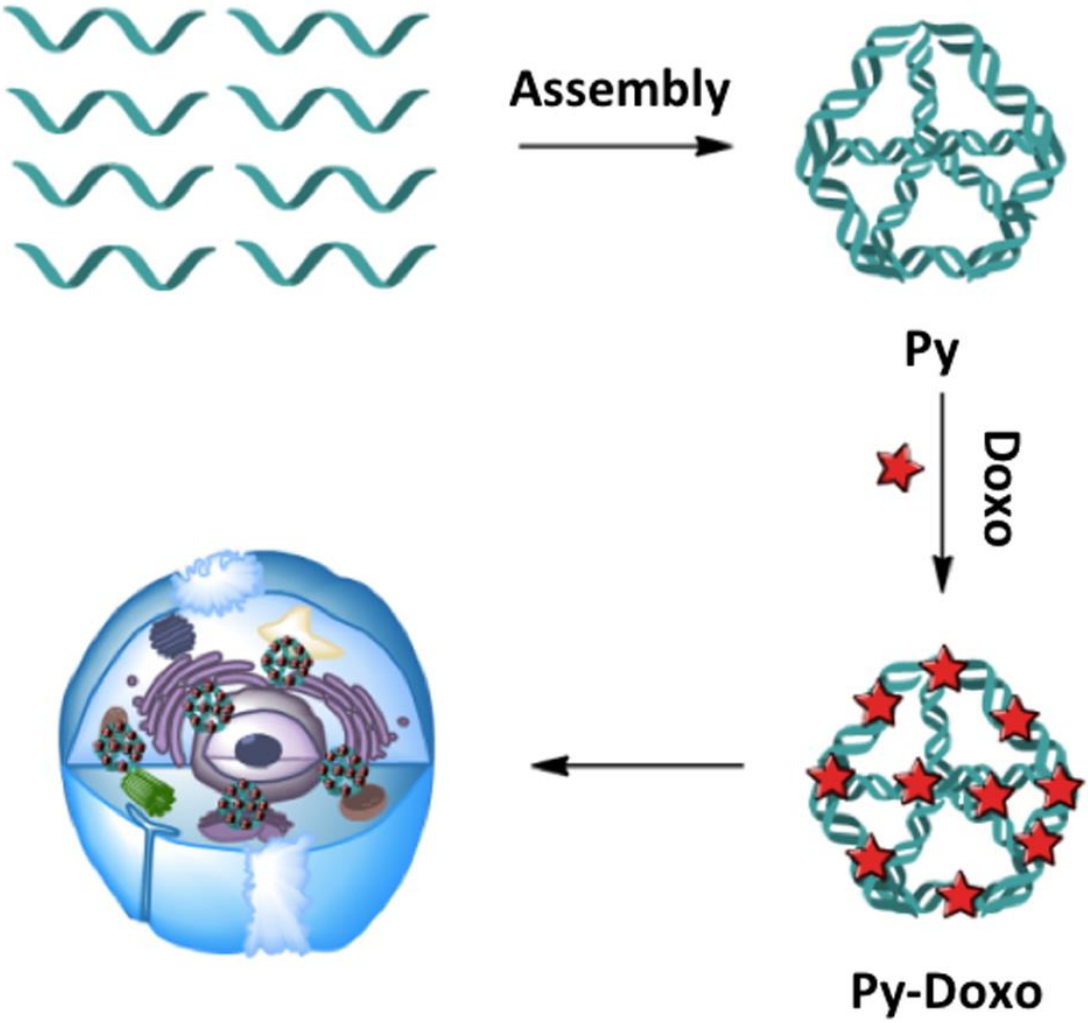

Scheme 1